Solar Physics (2023) 298:31
https://doi.org/10.1007/s11207-023-02123-8

RESEARCH

High-Energy Emissions Observed in the Impulsive Phase of the 2001 August 25 Eruptive Flare

Boris Y. Yushkov[1] · Victoria G. Kurt[1] · Vladimir I. Galkin[2,1]

Received: 5 December 2022 / Accepted: 6 February 2023

Abstract
We analyze here the impulsive phase of the 2001 August 25 eruptive flare (X5.3, S21, E38) in order to reveal the link of the time evolution of the magnetic-field reconnection rate $\dot{\varphi}(t)$ with the energy-release process, as quantified by electron and proton acceleration to high energies. Hard X-rays and γ-rays from 150 keV to 100 MeV were observed by the SONG (SOlar Neutrons and Gamma) detector onboard the CORONAS-F (Complex ORbital ObservatioNs of the Active Sun) mission. The soft X-ray derivative dI_{SXR}/dt was used as a proxy for the flare energy release that revealed itself as a sequence of acceleration pulses. The reconnection rate $\dot{\varphi}(t)$ was calculated previously from flare-ribbon observations in EUV and coaligned magnetic-field maps. The γ-ray emission spectra were obtained from SONG data. All spectra contain both bremsstrahlung and γ-ray lines. The bremsstrahlung spectrum extends to tens of MeV. The pion-decay gamma-ray emission, being a manifestation of proton acceleration to subrelativistic energies, appeared for the first time in the time interval of the $\dot{\varphi}(t)$ maximum. This maximum was ahead of the maxima of dI_{SXR}/dt as well as of all other emissions by about one minute. Proton acceleration to subrelativistic energies is confirmed by detection of solar neutrons by SONG and the Chacaltaya neutron monitor.

Keywords Acceleration, energetic particles · Flares · Magnetic reconnection · Spectrum · High-energy emissions

✉ B.Y. Yushkov
clef@srd.sinp.msu.ru

V.G. Kurt
vgk@srd.sinp.msu.ru

V.I. Galkin
v_i_galkin@mail.ru

1 Skobeltsyn Institute of Nuclear Physics, Lomonosov Moscow State University, Moscow, 119991, Russian Federation

2 Faculty of Physics, Lomonosov Moscow State University, Moscow, 119991, Russian Federation

Published online: 28 February 2023

1. Introduction

The development of a solar flare is governed by magnetic reconnection that provides a powerful energy release (e.g., Fletcher and Hudson, 2001; Longcope and Beveridge, 2007; Qiu et al., 2007; Miklenic et al., 2007). The so-called "standard flare model" (CSHKP, Carmichael, 1964; Sturrock, 1966; Hirayama, 1974; Kopp and Pneuman, 1976), which is a 2.5D approach with translation symmetry, successfully explains the morphology of eruptive flares, quasiparallel chromospheric ribbons and their movement in the course of a flare. Within the CSHKP framework, a magnetic-flux system can become unstable and at some point rise to higher coronal altitudes. A current sheet develops beneath them, towards which the ambient antiparallel magnetic field is brought in close contact and forced to reconnect (e.g., Priest and Forbes, 2000).

Observations of chromospheric Hα/extreme ultraviolet (EUV) flare ribbons and kernels as well as hard X-ray (HXR) footpoints (FPs) together with photospheric magnetograms were used in a number of studies for estimation of the total reconnected magnetic flux and reconnection rate in the impulsive phase of solar flares. According to the generalized 3D model (e.g., Longcope and Beveridge, 2007), magnetic reconnection that releases the stored energy and produces the flare ribbons also creates a flux rope. This fact leads naturally to a relationship of the reconnected flux and flare emissions.

On the basis of general considerations, it can be assumed that any energetically important reconnection process is accompanied by the acceleration of charged particles, which, in turn, are responsible for the appearance of microwave radiation, soft X-rays (SXR), HXR, and γ-rays. The fundamental force capable to accelerate a charged particle is caused by an electric field (see, e.g., Jokipii, 1979). Differences in the large-scale structure and time evolution of the accelerating electric field in terms of several basic scenarios are discussed by Zharkova et al. (2011). Electric fields can arise in a variety of ways, such as a potential drop at the reconnection site, turbulence, or different kinds of MHD shock waves produced during flares (e.g., the review by Miller et al., 1997). Specifically, Forbes and Lin (2000) considered the magnetic flux φ of single polarity swept by the flare ribbons and its time derivative $\dot{\varphi}(t)$ that gives the voltage drop along the magnetic-field polarity-inversion line (PIL) and corresponds to the conversion rate of the open flux to the closed one. Recently, there was a significant amount of interest in solar-flare studies to model particle acceleration in a single large-scale reconnection layer and in flare termination shocks (see, e.g., Kontar et al., 2017; Kong et al., 2022; Li et al., 2022) where turbulent energy can play a key role in the transfer of energy. The results show general agreement with certain observed electron spectra and emission signatures in the coronal region (see, e.g., Kong et al., 2022).

Electron beams are the main cause of the low-atmosphere heating and govern the behavior of emissions that are the visible manifestations of a flare impulsive phase development (e.g., Benz, 2008; Kontar et al., 2011; Aschwanden et al., 2017). In practice, the bremsstrahlung with photon energies of 20 – 25 keV is generally regarded as an indicator of the instantaneous rate of electron acceleration (Hudson, 1991; Dennis, Veronig, and Schwartz, 2003).

A significant source of information also comes from the observations of broadband radio (gyrosynchrotron) emission. This emission is produced by the gyromotion of electrons as they travel along coronal magnetic fields. The mechanism is extremely efficient and allows us to detect electrons with energies of hundreds of keV even in very small quantities (e.g., Klein, Trottet, and Magun, 1986; White et al., 2003; Nita, Gary, and Lee, 2004; Kuznetsov and Kontar, 2015). HXR and radio data combined with the Geostationary Operational Environmental Satellite (GOES) SXR data provide a useful qualitative representation – a proxy of the time evolution of energy release in the flare impulsive phase.

As far as we know, a thorough combined study of the time evolution of the magnetic-reconnection rate and the high-energy emission variations of a flare has not been carried out previously. In the present article, we discuss the peculiarities of these proxies alongside the high-energy electron bremsstrahlung, the γ-ray lines, and the π-decay γ-ray emission observed in the impulsive phase of the 2001 August 25 eruptive flare. We shall concentrate on the interrelationship of the reconnection-rate time behavior and the particle acceleration to high energies.

The article is structured in the following way. A brief overview of the 2001 August 25 flare is presented in Section 2. Comparison of reconnected magnetic flux and flare emissions is presented in Section 3. In Section 4, observations of high-energy gamma-rays and neutrons are discussed. Section 5 summarizes the results and discusses them.

2. Overview of the Flare Impulsive Phase

The eruptive SOL2001-08-25 flare (X5.3/3B) occurred in NOAA Active Region 9591 at S21, E38 and was observed by a number of observatories and instruments in microwave, Hα, EUV, X-ray, and γ-ray ranges. Hard X-ray Telescope (HXT) and Gamma-Ray Spectrometer (GRS) detectors installed onboard the Yohkoh have measured emission from 22 keV up to 8 – 30 MeV (Kosugi et al., 1991; Ogawara et al., 1991; Sato et al., 2006). Metcalf et al. (2003) studied the flare using the data of Transition Region and Coronal Explorer (TRACE, Handy et al., 1999) white-light channel and Yohkoh HXT. The flare was also observed by Konus-Wind (http://www.ioffe.ru/LEA/kwsun/). A brief description of solar-flare observations by this mission can be found in Lysenko et al. (2018). Grechnev, Kochanov, and Uralov (2023) studied the evolution of coronal mass ejection (CME) and a shock wave in this eruptive event. Kuznetsov et al. (2006) and Kurt et al. (2010, 2013) reported that the SONG (SOlar Neutrons and Gamma) detector (Kuznetsov et al., 2011) onboard the CORONAS-F (Complex ORbital ObservtioNs of the Active Sun) mission observed high-energy gamma-ray emission up to 100 MeV including the π-decay γ-rays during the flare impulsive phase. Solar neutrons were also measured by SONG and the high-altitude neutron monitor (NM) Chacaltaya (Watanabe et al., 2003) during the same event. Here, we present the available diagnostic data of the impulsive phase of this flare from the start. Combined observations allowed us to follow in detail the evolution of the flare emissions.

Figure 1 presents the profiles of the flare emissions observed in several energy ranges. Background values were subtracted. The data demonstrate that the Neupert effect revealed itself both in its classic form that established a link between microwaves and SXR (Neupert, 1968) and in its modern interpretation (e.g., Dennis and Zarro, 1993; Veronig et al., 2005; Benz, 2008). The latter implies the following connection of HXR and SXR fluxes:

$$\frac{d}{dt} F_{\mathrm{SXR}}(t) \propto F_{\mathrm{HXR}}(t). \tag{1}$$

Hence, we will use hereinafter the GOES SXR derivative, dI_{SXR}/dt as an indicator of the flare energy release. The flare onset was indicated by NOAA, Space Environment Center in GOES-8 SXR at $\approx$ 16:23 UT. This time will be denoted T_0. The flux in the 1 – 8 Å GOES channel increased throughout the presented time interval and reached its maximum of 5.3×10^{-4} W m^{-2} at 16:45 UT. The increase of the microwave emission flux at 15.4 GHz observed by the Sagamore Hill Station (ftp://ftp.ngdc.noaa.gov/STP/space-weather/solar-data/solar-features/solar-radio/rstn-1-second/sagamore-hill/2001/08/) starting at $\approx$ 16:23:30 UT

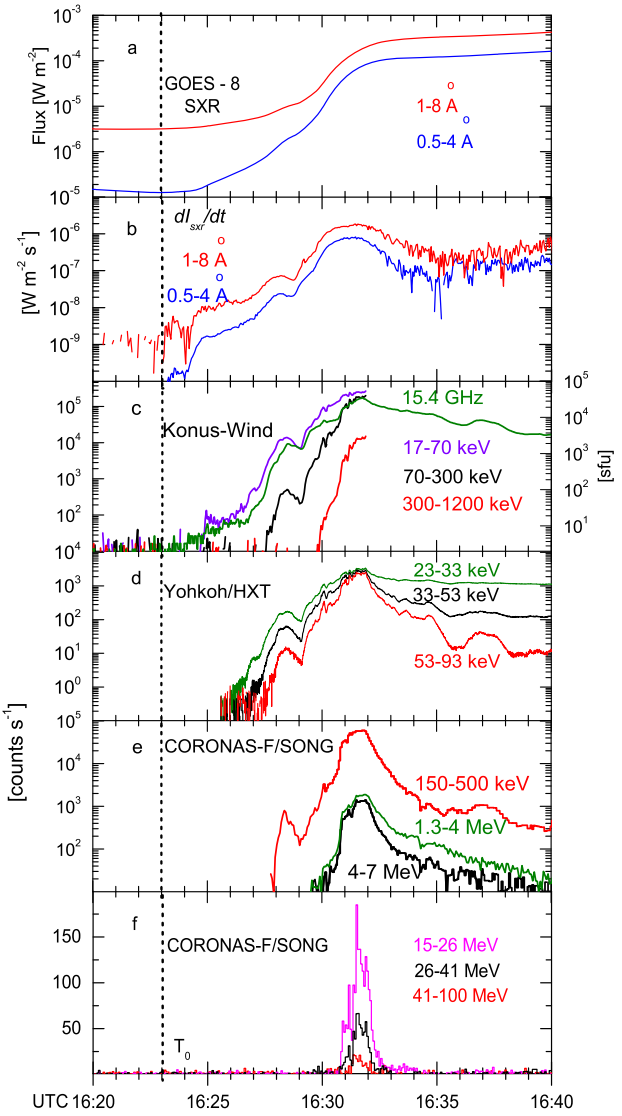

Figure 1 Emissions during the impulsive phase of the 2001 August 25 flare. **a**) SXR observed by GOES; **b**) SXR time derivatives; **c**) HXR observed by Konus-Wind and radio emission (olive curve, right Y-axis); **d**) HXR observed by Yohkoh/HXT; **e**) and **f**) gamma-ray emissions observed by CORONAS-F/SONG. Dashed vertical line indicates the flare onset T_0.

(see Figure 1c), suggested that the real onset of the intermediate-energy electron acceleration was close to T_0. The Konus-Wind detector measured the HXR increase above the background in the 17 – 70 keV channel at ≈ 16:25:00 UT. The records were interrupted at 16:31:55 UT due to memory overflow. The Yohkoh records switched from the "quiet mode" to the "flare mode" only at 16:25:34 UT. From this moment, Yohkoh/HXT began to observe the flare emission of accelerated electrons. Panels e and f of Figure 1 present γ-ray emission observed by CORONAS-F/SONG. Figure 1 demonstrates the consistency of all the presented measurements over a wide range of photon energies. A full agreement between the data of the various detectors was observed including a weak feature at ≈ 16:30 UT. The absence of overloads and other possible distortions of the data in this powerful flare has been shown. Due to this, we conclude that observed time profiles reflect the evolution of the flare emissions.

Measurements of the emission by a variety of detectors covering a wide range of energies from microwaves to 100 MeV γ-rays made it possible to follow the time sequence of particle acceleration while this flare was in progress. Figure 1 shows the most pronounced episodes of particle acceleration:

- the microwave emission indicated that the first pulse of electron acceleration apparently up to 100 – 150 keV occurred between 16:23:00 UT and 16:24:00 UT;
- however, the detectors of HXR emission could establish the availability of the electrons with energies above 20 keV only from 16:25:00 UT;
- the minor peaks between 16:28 UT and 16:29 UT were seen in the radio emission and in HXR profiles;
- the main pulse of acceleration started at 16:29 UT with the increase of HXR to 300 keV;
- γ-rays with energies > 1.3 MeV were observed from 16:30 UT;
- increase of the count rates in the 15 - 26 MeV and higher SONG channels occurred after 16:30:44 UT;
- HXR and γ-ray emissions fluxes after 16:32:00 UT decreased with two weak, but distinct, acceleration episodes at about 16:35 UT and 16:37 UT.

Thus, flare energy release revealed itself as the sequence of particle-acceleration pulses with the increasing photon energy and reached a maximum at about 16:31:30 – 16:32 UT. After this point, the acceleration efficiency of high-energy particles dropped sharply.

3. Reconnected Magnetic Flux and Flare Emissions

Reconnection process in the corona cannot be observed directly, but can be tracked via the temporal and spatial evolution of flare ribbons observed in EUV and in the Hα line. HXR, EUV, and Hα emissions are produced by the precipitated electrons. These emissions rise and reach peak levels almost simultaneously on very short time scales. The ribbon apparent motion is obviously due to the spread of reconnection along adjacent field lines, leading to energy deposition and heating of the atmosphere at the feet of newly reconnected field lines.

A certain correlation has been established between the time evolution of the magnetic-field reconnection rate, the time profiles of SXR derivative or HXR emission in the flare impulsive phase (e.g., Qiu, 2009; Miklenic, Veronig, and Vršnak, 2009; Veronig and Polanec, 2015). In the confined flare of 2014 October 22 (X1.6) Veronig and Polanec (2015) showed that the RHESSI HXR count rates reached a peak level within a one-minute interval close to the maximum of the reconnection rate. Conversely Miklenic, Veronig, and Vršnak (2009) found that the reconnection rate maximum in eruptive flares is observed somewhat ahead (1 – 2 min) of the main peak in the HXR. A similar time lag of the maximum of the SXR derivative relative to the reconnection rate maximum was also observed by Qiu (2009) based on EUV data.

Figure 2a presents the reconnected magnetic fluxes $\varphi(t)$. Points were computed from the observations of chromospheric EUV flare ribbons using the TRACE 284 Å images together with the vertical magnetic field extrapolated to a height of 1.4 Mm in the potential-field approximation from the photospheric line-of-sight magnetograms (Grechnev, Kochanov, and Uralov, 2023). The amount of magnetic flux that took part in the reconnection process till 16:40 UT was found to be 7.2×10^{21} Mx. Probable measurement errors for the averaged reconnected magnetic flux are within $\pm 30\%$ (Grechnev, Kochanov, and Uralov, 2023).

The magnetic-flux change rate $\dot{\varphi}(t)$ presented in Figure 2b was computed separately for each magnetic polarity as the time derivative of the reconnected flux $\varphi(t)$; in so doing the

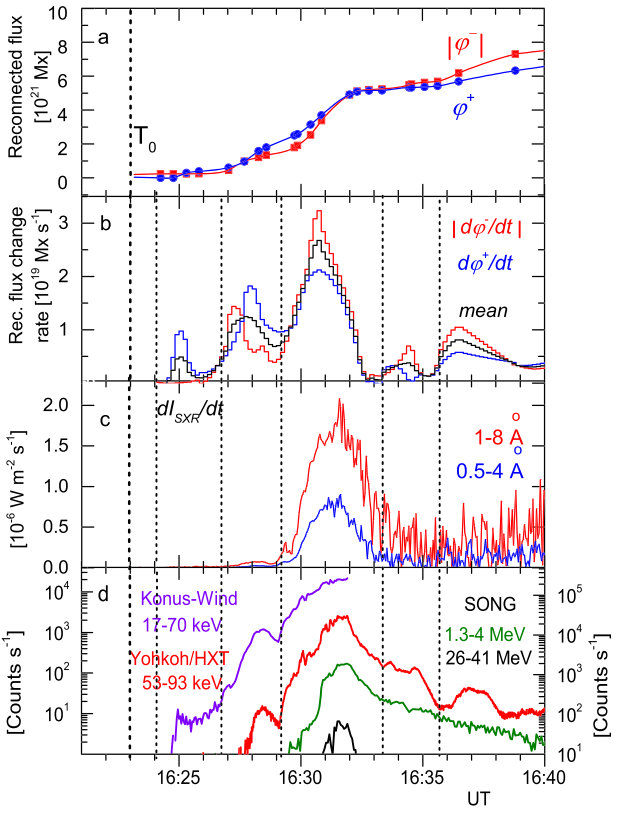

Figure 2 Comparison of the reconnected flux with the SXR, HXR, and gamma-ray emissions in the 2001 August 25 flare. **a**) reconnected magnetic fluxes $\varphi(t)$; **b**) their derivatives $\dot{\varphi}(t)$. The black line presents the mean of two polarities. **c**) GOES SXR derivatives; **d**) the HXR and γ-ray count rates observed by Yohkoh/HXT (red curve, left Y-axis), Konus-Wind (blue), and SONG (both right Y-axis). Dashed thick vertical line indicates the flare onset T_0. Short-dashed vertical lines denote the beginning of the most pronounced episodes of acceleration (energy release).

flux was calculated using the four-point Lagrange interpolation formula with 10-s steps. The mean maximum $\dot{\varphi}(t)$ was equal to 2.7×10^{19} Mx s^{-1} between 16:30:30 and 16:31:00 UT. Unfortunately, a large gap in flux data does not permit us to determine more exactly the time of this maximum. Tschernitz et al. (2018) found the peak reconnection rate in this flare to be 1.5×10^{19} Mx s^{-1} based on Hα observations.

Figure 2 shows clearly that particle acceleration/energy release happened as several separate episodes of 2 – 3 min duration marked by short-dashed vertical lines. From the standard flare model, it is expected that each significant episode of particle acceleration/energy release occurred simultaneously with each episode of the reconnection rate change. Indeed, such a coincidence is seen in several moderate pulses. However, the main peak of energy release at $\approx$ 16:31:45 UT appeared obviously later than the $\dot{\varphi}(t)$ maximum observed at $\approx$ 16:30:40 UT although both increases started simultaneously. Comparison of panels 2b and 2c shows that the energy release did not depend linearly on the reconnection rate.

The high intensity of the emissions observed in the vicinity of the $\dot{\varphi}(t)$ maximum allowed us to study their behavior with high time resolution having high statistical accuracy. Figure 3 shows the time interval zoomed to 16:29 – 16:33 UT. The time interval ΔT_1 of 16:30:30 – 16:31:00 corresponds to $\dot{\varphi}(t)$ values of $\geq$ 90% of maximum. The time interval ΔT_2 of 16:31:20 – 16:31:56 UT corresponds to maximum values of the GOES SXR derivative smoothed over 10 points. Figure 3 also presents data on the γ-ray emission obtained from SONG observations that had 4-s time resolution combined with data of the Yohkoh HXT and GRS detectors having 1-s time resolution and the Konus-Wind data with 3-s reso-

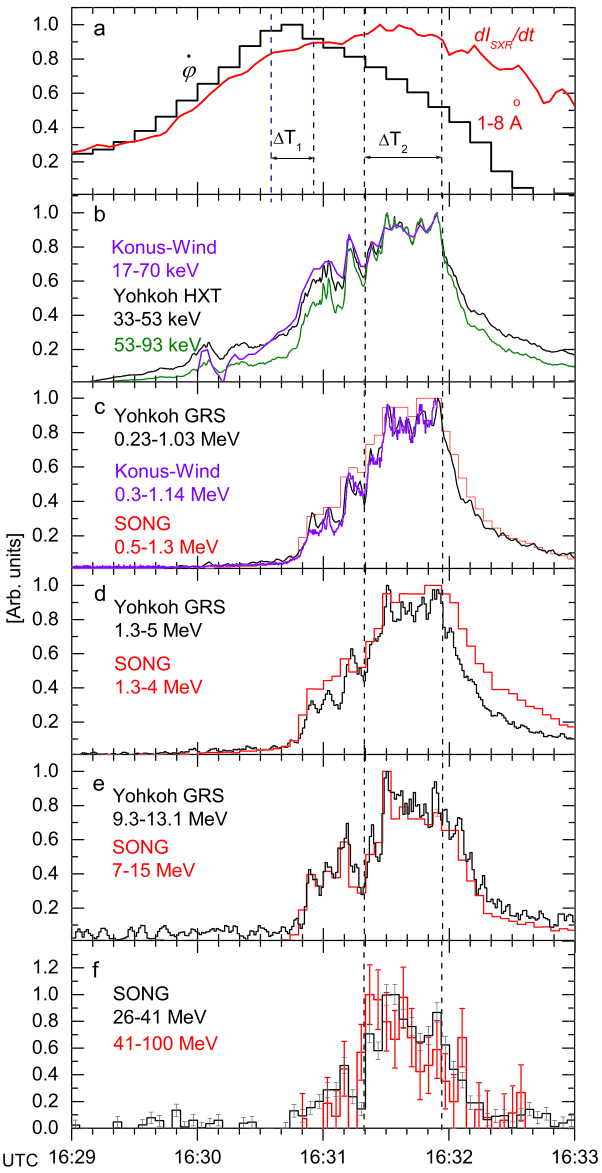

Figure 3 Emissions in the vicinity of the impulsive phase maximum of the 2001 August 25 flare. **a**) the $\dot{\varphi}(t)$ evolution (black) and GOES SXR derivative (red); **b**–**f**) data of different observations. All curves were background subtracted and normalized to maxima.

lution. Figure 3, as well as Figure 1, demonstrates the high consistency of measurements in the overlapping energy channels visible, even in a fine structure at the time scale of several seconds.

The first maxima of HXR and γ-ray up to 7 – 15 MeV were observed at 16:31:30 UT $\pm$2 s. Then, the second peak of these emissions occurred at about 16:31:54 UT when the reconnection rate has already significantly decreased. Figure 14 of Metcalf et al. (2003) allows us to assume that both mentioned peaks were characterized by approximately the same values of thick target HXR power above 20 keV. Given that the bulk of the released energy occurred in the low-energy part of electron spectrum at 20 – 25 keV (e.g., Emslie et al.,

2012; Aschwanden et al., 2017), we can say that the flare energy release took place at $\geq 90\%$ of maximum level in the interval ΔT_2. Maxima of all HXR and γ-ray emissions including energies of 41 – 100 MeV were also observed in this interval. Hence, we confidently assert that maximum of energy release and the most efficient particle acceleration were delayed regarding the reconnection-flux change-rate maximum for about one minute. This delay is consistent with values found in the eruptive flares by Qiu (2009) and Miklenic, Veronig, and Vršnak (2009).

Further consideration will be focused on the study of changes in the spectral composition of the observed high-energy emission over the crucial time intervals of the flare development.

4. High-Energy Gamma-Rays and Neutrons

Accelerated ions constitute an energetically important component of a flare as well. In contrast to the nonthermal electrons, which produce HXR only in a single process, namely the bremsstrahlung, accelerated protons/ions contribute to the flare emission via distinct processes observable in the γ-ray energy domain. Protons with energies < 10 MeV and between 100 and 300 MeV are invisible in the solar atmosphere because there are no significant nuclear reactions to create γ-rays. Information of the ion acceleration up to 10 – 100 MeV is based on observations of γ-ray lines in the 2 – 7 MeV energy range (e.g., Vilmer, MacKinnon, and Hurford, 2011). The appearance of protons with energies $\geq$ 300 MeV in the solar atmosphere can be identified by the emergence of a specific feature in the spectrum of high-energy γ-ray emission. This spectral feature is caused by the decay of neutral and charged pions, which in their turn are produced in the interactions of protons of energies above the threshold of ≈ 300 MeV with dense layers of the solar atmosphere (e.g., Murphy and Ramaty, 1984; Ramaty and Murphy, 1987; Murphy, Dermer, and Ramaty, 1987). Charged pions produce muons and ultimately electrons and positrons, which, in turn, generate high-energy bremsstrahlung with an energy spectrum extending up to the energies of parent electrons and positrons. Neutral pions generate a broad γ-ray line with the maximum near 70 MeV. The resulting spectrum is characterized by a specific plateau at 30 – 100 MeV. No other process can produce a spectral feature similar to the pion-decay gamma-ray emission. Observation of this emission in a solar event ascertains the proton acceleration up to subrelativistic energies.

When high-energy protons interact with matter, γ-line and pion-decay γ-rays are emitted almost instantaneously. Observation of these emissions thus makes it possible to follow the time behavior of high-energy protons in the solar atmosphere (e.g., Vilmer, MacKinnon, and Hurford, 2011). To specify the details of variations in composition and spectral characteristics of the flare emissions with time, we restored the spectra of an incident flare γ-ray emission. To do this we fitted the SONG energy-loss spectra with a three-component model: 1) the bremsstrahlung from primary accelerated electrons, 2) the broad continuum formed by prompt γ-ray line emission from nuclear deexcitation, and 3) the broad continuum produced by the pion-decay γ-ray emission. For the latter component, we used a simulated spectrum for a downward isotropic distribution of primary accelerated ions (R. Murphy, private communication). The bremsstrahlung spectrum is assumed to be a power-law function with a roll-over at high energies:

$$F(E) = I_0 E^{-\gamma} \exp\left(-\frac{E}{E_0}\right). \tag{2}$$

Table 1 Results of the spectral analysis.

Time, UT	Bremsstrahlung		γ-line flux at 5 MeV	π-decay emission flux at 100 MeV	Proton spectrum index
	γ	Flux at 150 keV			
16:28:00 – 16:30:00	4.0	$(2.0 \pm 0.3) \times 10^{1}$	$(3.9 \pm 1.0) \times 10^{-3}$	0	–
16:30:00 – 16:30:40	3.2	$(2.7 \pm 0.7) \times 10^{2}$	$(4.6 \pm 1.5) \times 10^{-2}$	$< 1.0 \times 10^{-5}$	–
16:30:40 – 16:31:20	2.6	$(1.8 \pm 0.2) \times 10^{3}$	$(4.0 \pm 1.5) \times 10^{-1}$	$(9.3 \pm 3.1) \times 10^{-4}$	3.7 ± 0.2
16:31:20 – 16 31:40	2.4	$(3.1 \pm 0.2) \times 10^{3}$	$(7.1 \pm 2.0) \times 10^{-1}$	$(5.2 \pm 1.4) \times 10^{-3}$	3.4 ± 0.2
16:31:40 – 16 32:00	2.3	$(3.0 \pm 0.2) \times 10^{3}$	$(6.0 \pm 1.8) \times 10^{-1}$	$(3.3 \pm 1.1) \times 10^{-3}$	3.5 ± 0.2
16:32:00 – 16:33:00	2.5	$(9.8 \pm 2.0) \times 10^{2}$	$(6.4 \pm 2.2) \times 10^{-1}$	$(8.2 \pm 2.8) \times 10^{-4}$	3.8 ± 0.2

*Fluxes in the third–fifth columns are given in photon $\mathrm{cm}^{-2}\,\mathrm{s}^{-1}\,\mathrm{MeV}^{-1}$.

As the SONG detector had 12 broad energy channels, it could not discriminate narrow gamma-ray lines including the well-known neutron-capture line at 2.223 MeV. We employed in the fitting procedure a broad continuum in the 0.5 – 12 MeV energy range produced by the superposition of these lines. The continuum was built up on the basis of Murphy et al. (2009) data. The response matrices of the SONG detector were simulated using the GEANT 3.21 separately for each spectral component mentioned above. The uniquely available Yohkoh/GRS spectrum at 16:31:38 – 16:31:58 UT (http://ylstone.physics.montana.edu/ylegacy/) did not reveal the 2.223 MeV line. Based on this data we assumed that the contribution of this line to SONG channel count rates could be considered negligible.

The fitting was performed using the SONG channels above 150 keV. The main results of the performed spectral analysis are summarized in Table 1.

Each SONG spectrum contains both bremsstrahlung and γ-ray lines. Fitted values of E_0 were above 40 MeV in all spectra. These values affect weakly the fit results. The current three-component model allowed us to determine fluxes of γ-ray lines and bremsstrahlung with higher accuracy than the values presented in Kurt et al. (2013). The pion-decay γ-ray fluxes were not noticeably changed.

Figure 4 presents several restored spectra. Reasonable agreement of SONG and Yohkoh spectra at 16:31:40 – 16:32:00 UT is evident. The bremsstrahlung extends up to tens of MeV during the main energy release that confirms electron acceleration up to ultrarelativistic energies. Such high energies can be explained by values of electric field about 30 $\mathrm{V\,cm}^{-1}$ calculated in this flare by Hinterreiter et al. (2018).

With the help of our fitting procedure we managed to extract a statistically significant flux of the π-decay γ-ray emission after 16:30:40 UT, when the reconnection rate was going through the 90% level of the maximum found between 16:30:30 and 16:31:00 UT (see Table 1). The spectrum accumulated between 16:31:20 and 16:31:40 UT, corresponds to the pion-decay γ-ray emission maximum. Maximum fluxes of both bremsstrahlung and γ-ray lines were also observed in this time interval.

The spectral hardness of accelerated ions can be studied through comparison of different components of fluxes of the γ-ray emission, namely prompt nuclear γ-ray lines in the 4 – 7 MeV range, F_{4-7}, and the π-decay γ-ray emission in the 30 – 100 MeV range, F_{π}, because these components are produced by particles belonging to different energy ranges (Ramaty and Murphy, 1987). To estimate the power-law index S of the proton spectrum we used the S dependence on the F_{π}/F_{4-7} ratio calculated for the downward isotropic distribution of primary accelerated ions (see Figure 4 in Dunphy et al., 1999). We calculated F_{π}/F_{4-7} ratios using these fluxes obtained from the SONG spectra. The power-law index S of the proton spectrum is presented in Table 1. Irrespective of the large errors of the S calculation

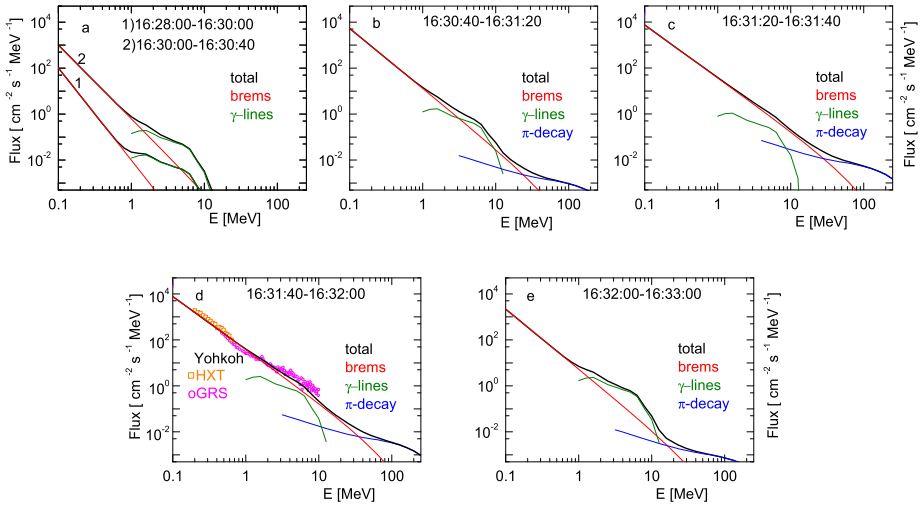

Figure 4 Flare gamma-ray spectra restored from the SONG data for successive acceleration episodes. Black curves present the total spectrum, red – the bremsstrahlung component, olive – γ-ray lines, blue – π-decay gamma-ray emission. The spectra taken from the Yohkoh GRS flare catalog (http://ylstone.physics.montana.edu/ylegacy/) are presented in panel **d** as points.

we believe that the strongest proton spectrum was observed at 16:31:20 – 16:32:00 UT, i.e., during the maximum of the π-decay gamma-ray emission.

High-energy protons that produce pions also generate high-energy neutrons in the same p–p and p–α interaction with solar matter. Pions decay almost instantly and produce γ-rays with a specific spectrum. Neutrons can escape the Sun and reach the Earth. The velocity of the main bulk of these neutrons is lower than the speed of light, so neutrons should arrive delayed as compared to the simultaneously generated γ-rays. The value of the time delay allows estimation of the energy of neutrons and, therefore, of the 'parent' proton's energy. Note that the time profile of the observed neutron flux is essentially extended due to both velocity dispersion and inflight decay as compared to the γ-ray emission time profile that is directly coupled to the time evolution of high-energy proton interactions.

High-energy solar neutrons were observed in the 2001 August 25 event by SONG (Kuznetsov et al., 2006) and also by the NM installed at Mt. Chacaltaya, Bolivia (Watanabe et al., 2003). Evidence of neutron detection was recorded by SONG at 16:34:30 UT $\pm$30 s and by Chacaltaya NM between 16:35:00 and 16:36:00 UT (see Figure 5). Figure 5 also contains the time profile of high-energy γ-rays that allowed us to estimate the time delay of neutrons to be $\approx$ 3 min and to estimate their energy. Both SONG and Chacaltaya NM data provided similar values of neutron energy to be above $\approx$ 500 MeV. This means that protons were accelerated at the Sun to energies above 1 GeV (see Figure 9 from Murhpy, Dermer, and Ramaty, 1987). This energy corresponds to the high values of the cross section of pion production. Watanabe et al. (2003) estimated a power-law index of the neutron spectrum at the Sun as 3.9 ± 0.7 that is consistent with the estimated spectrum index of parent protons (see Table 1). Along with observation of the pion-decay γ-rays, detection of high-energy solar neutrons is additional and independent evidence of proton acceleration to subrelativistic energies in this flare. Neither Ground Level Enhancement nor Solar Proton Event was observed after this eastern-hemispheric flare (see http://www01.nmdb.eu/nest; Kurt et al., 2004; Vainio et al., 2013).

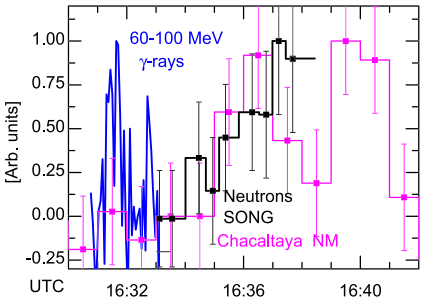

Figure 5 High-energy γ-rays observed by SONG (blue), and neutrons observed by SONG (black curve) and Chacaltaya NM (magenta) on 2001 August 25. Background values were subtracted.

5. Summary and Discussion

We focused in our study on the time behavior of the emissions measured during the impulsive phase of the 2001 August 25 flare. We used data from several detectors covering a broad energy range. Good agreement of these data proves that the observed time profiles really represent the flare emission evolution. Our findings are:

i) The flare energy release, observed via the emissions, took place as a sequence of the acceleration pulses. Close resemblance of the time courses of the flare manifestations: $\dot{\varphi}(t)$ and $dI_{\mathrm{SXR}}/dt\,(t)$ was obtained. The beginnings of each pulse of both processes occurred at the same time. All peaks of both curves except the highest ones also occurred at the same time points. The reconnection rate at 90% of the maximum level was between 16:30:30 and 16:31:00 UT. This maximum was observed about one minute ahead of the energy-release maximum. This delay qualitatively agrees with the earlier results by Qiu (2009) and Miklenic, Veronig, and Vršnak (2009) concerning eruptive flares.

ii) We performed spectral analysis of the flare emission measured by SONG in the 150 keV – 100 MeV energy range and derived the principal characteristics and composition of the emission in six successive time intervals. All flare spectra contain both γ-ray lines and bremsstrahlung. The exceptionally intense flux of bremsstrahlung observed at high confidence level up to tens of MeV confirms electron acceleration to ultrarelativistic energies during the main energy release. This is a unique case till now in which bremsstrahlung of such high energies was detected in a flare main energy-release phase.

iii) The observation of the pion-decay gamma-ray emission proves the proton acceleration of $\geq$ 300 MeV. The beginning of this emission was observed at 16:31:00 UT $\pm$20 s, whereas a reconnection rate at the 90% level has been indicated at 16:30:45 UT $\pm$15 s. Apparently, protons needed few extra seconds to gain energy above the pion-production threshold. The maximum of the pion-decay γ-rays was observed within the time interval of the main energy release.

iv) Proton acceleration to subrelativistic energies in the flare was confirmed by detection of solar neutrons by SONG and the Chacaltaya NM.

All these results, taken together, prove that the change of the acceleration regime occurred at the crucial interval of the reconnection rate evolution in the 25 August 2001 flare. Magnetic reconnection governs the course of the flare. Grechnev, Kochanov, and Uralov (2023) found in this event a close relationship between the reconnection rate and acceleration of the erupting flux rope that became the CME, and the most energetic part of the flare that manifested in the strongest HXR and γ-ray emissions. The existence of the delay of the maximum energy release relative to time of the maximum magnetic-field reconnection rate is probably an intrinsic property of the flare associated with CME.

The emission as a function of time is a complex superposition of particle-acceleration processes, transport, and energy loss in the subcoronal segments. The total timescale of these processes is much shorter than the time resolution of EUV data used to derive the reconnection rates. If we take this into account then the relationship between the acceleration itself and the reconnection rate $\dot{\varphi}(t)$ changes can be even closer. It is likely that the onset time of the pion-decay γ-ray emission somehow demarcates time intervals with different signatures of charged-particle acceleration.

No data were available on vertical distribution of the coronal magnetic field structure in the 2001 August 25 flare. There were also no data on direct observations of coronal HXR sources. However, we speculate that the flare main energy release and proton acceleration up to subrelativistic energies started in the regions of cusp location and at the bottom of the reconnection current sheet created after a significant change in the topology of the flare affected by the CME-associated magnetic flux-rope eruption.

An additional indirect argument in favor of such an assumption is: all flares known to us in the impulsive phase of which the pion-decay gamma-ray emission was detected before Fermi-LAT era were eruptive. Fermi-LAT convincingly proved such an association (see Figure 26 in Ajello et al., 2021). In particular, the flare on 2010 June 12 (Ackermann et al., 2012), with the lowest importance M2 among all other flares with π-decay γ-rays was associated with CME.

Acknowledgments We thank the anonymous referee for a very helpful and constructive review. We wish to acknowledge V.V. Grechnev, A.A. Kochanov, and A.M. Uralov whose calculations of reconnected magnetic flux in this flare are decisive in this paper. We also thank them for helpful advice and discussions. We appreciate the science and instrument teams of Yohkoh, GOES, CORONAS-F, and Konus-Wind. We are especially grateful to A.L. Lysenko for providing detailed measurements of this flare with the Konus instrument.

Author contributions B.Yu. Yushkov: primary data processing, development of spectra restoration method and its realization, scientific analysis of data, discussion of results and manuscript preparation. V.G. Kurt: main scientific analysis of data, discussion of results and manuscript preparation. V.I. Galkin: principal development of spectra restoration method and its realization, scientific analysis of data, discussion of results.

Funding The study was carried out within the state budget topic no. 122071200023-6 for SINP MSU.

Data Availability The datasets analyzed during the current study were derived from the following public-domain resources: Yohkoh Legacy data Archive http://ylstone.physics.montana.edu/ylegacy/; Konus-Wind Solar Flare Database http://www.ioffe.ru/LEA/kwsun/; RSTN data ftp://ftp.ngdc.noaa.gov/STP/space-weather/solar-data/solar-features/solar-radio/ NOAA, Space Environment Center; ftp://ftp.ngdc.noaa.gov/STP/space-weather/solar-data/solar-features/solar-radio/rstn-1-second/sagamore-hill/2001/08/. The CORONAS-F/SONG data are available from the corresponding author on reasonable request.

Declarations

Competing interests The authors declare no competing interests.

References

Ackermann, M., Ajello, M., Allafort, A., Atwood, W.B., Baldidi, L., Barbellini, G., et al.: 2012, Fermi detection of γ-ray emission from the M2 soft X-ray flare on 2010 June 12. *Astrophys. J.* **745**, 144. DOI. ADS.

Ajello, M., Baldini, L., Bastieri, D., Bellazzini, R., Berretta, A., Bissaldi, E., et al.: 2021, First Fermi-LAT solar flare catalog. *Astrophys. J. Suppl.* **252**, 13. DOI. ADS.

Aschwanden, M.J., Caspi, A., Cohen, C.M.S., Holman, G., Jing, J., Kretzschmar, M., Kontar, E., et al.: 2017, Global energetics of solar flares. V. Energy closure in flares and coronal mass ejections. *Astrophys. J.* **836**, 17. DOI. ADS.

Benz, A.: 2008, Flare observations. *Living Rev. Solar Phys.* **5**, 1. DOI. ADS.
Carmichael, H.: 1964, A process for flares. *NASA Spec. Publ.* **50**, 451.
Dennis, B.R., Zarro, D.M.: 1993, The Neupert effect – what can it tell up about the impulsive and gradual phases of solar flares. *Solar Phys.* **146**, 177. DOI. ADS.
Dennis, B., Veronig, A., Schwartz, R.: 2003, The Neupert effect and new RHESSI measures of the total energy in electrons accelerated in solar flares. *Adv. Space Res.* **32**, 2459.
Dunphy, P., Chupp, E., Bertsch, D.L., Schneid, E.J., Gottesman, S.R., Kanbach, G.: 1999, Gamma-rays and neutrons as a probe of flare proton spectra: the solar flare of 11 June 1991. *Solar Phys.* **187**, 45. DOI. ADS.
Emslie, G., Dennis, B.R., Shih, A.Y., Chamberlin, C., Mewaldt, R.A., Moore, C.S., Share, G.H., Vourlidas, A., Welsch, B.T.: 2012, Global energetics of thirty-eight large solar eruptive events. *Astrophys. J.* **799**, 71. DOI. ADS.
Fletcher, L., Hudson, H.: 2001, The magnetic structure and generation of EUV flare ribbons. *Solar Phys.* **204**, 69. DOI. ADS.
Forbes, T.G., Lin, J.: 2000, What can we learn about reconnection from coronal mass ejections? *J. Atmos. Solar-Terr. Phys.* **62**, 1499.
Grechnev, V.V., Kochanov, A.A., Uralov, A.M.: 2023, The 25 August 2001 high-energy solar event. Eruptive flare, CME, and shock wave. *Solar Phys.* in press.
Handy, B.N., Acton, L.W., Kankelborg, C.C., Wolfson, C.J., Akin, D.J., Bruner, M.E., et al.: 1999, The transition region and coronal explorer. *Solar Phys.* **187**, 229.
Hinterreiter, J., Veronig, A.M., Thalmann, J.K., Tschernitz, J., Pötzi, W.: 2018, Statistical properties of ribbon evolution and reconnection electric fields in eruptive and confined flares. *Solar Phys.* **293**, 38. DOI. ADS.
Hirayama, T.: 1974, Theoretical model of flares and prominences. I. Evaporating flare model. *Solar Phys.* **34**, 323. DOI. ADS.
Hudson, H.S.: 1991, Solar flares, microflares, nanoflares, and coronal heating. *Solar Phys.* **133**, 357. DOI. ADS.
Jokipii, J.R.: 1979, *Particle Acceleration Mechanisms in Astrophysics*, *AIP Conf. Proc.* **56**, AIP, La Jolla, 1.
Klein, K.-L., Trottet, G., Magun, A.: 1986, Microwave diagnostics of energetic electrons in flares. *Solar Phys.* **104**, 243.
Kong, X., Chen, B., Guo, F., Shen, C., Li, X., Ye, J., Zhao, L., Jiang, Z., Yu, S., Chen, Y., Giacalone, J.: 2022, Numerical modeling of energetic electron acceleration, transport, and emission in solar flares: connecting loop-top and footpoint hard X-ray sources. *Astrophys. J.* **941**, L22.
Kontar, E.P., Brown, J.C., Emslie, A.G., Hajdas, W., Holman, G., Hurford, G., Kašparová, J., et al.: 2011, Deducing electron properties from hard X-ray observations. *Space Sci. Rev.* **159**, 301. DOI. ADS.
Kontar, E.P., Perez, J.E., Harra, L.K., Kuznetsov, A.A., Emslie, A.G., Jeffrey, N.L.S., Bian, N.H., Dennis, B.R.: 2017, Turbulent kinetic energy in the energy balance of a solar flare. *Phys. Rev. Lett.* **118**, 155101.
Kopp, R.A., Pneuman, G.W.: 1976, Magnetic reconnection in the corona and the loop prominence phenomenon. *Solar Phys.* **50**, 85.
Kosugi, T., Makishima, K., Murakami, T., Sakao, T., Dotani, T., Inda, M., Kai, K., et al.: 1991, The Hard X-ray Telescope (HXT) for the SOLAR-A mission. *Solar Phys.* **136**, 17. DOI. ADS.
Kurt, V., Belov, A., Mavromichalaki, H., Gerontidou, M.: 2004, Statistical analysis of solar proton events. *Ann. Geophys.* **22**, 2255.
Kurt, V.G., Yushkov, B.Yu., Kudela, K., Galkin, V.I.: 2010, High-energy gamma radiation of solar flares as an indicator of acceleration of energetic protons. *Cosm. Res.* **48**, 70.
Kurt, V., Kudela, K., Yushkov, B., Galkin, V.: 2013, On the onset time of several SPE/GLE events: indications from high-energy gamma-ray and neutron measurements by CORONAS-F. *Adv. Astron.* **2013**, 690921. DOI. ADS.
Kuznetsov, A.A., Kontar, E.P.: 2015, Spatially resolved energetic electron properties for the 21 May 2004 flare from radio observations and 3D simulations. *Solar Phys.* **290**, 79.
Kuznetsov, S.N., Kurt, V.G., Myagkova, I.N., Yushkov, B.Yu., Kudela, K.: 2006, Gamma-ray emission and neutrons from solar flares recorded by the SONG instrument in 2001 – 2004. *Solar Syst. Res.* **40**, 104. DOI. ADS.
Kuznetsov, S.N., Kurt, V.G., Yushkov, B.Yu., Kudela, K., Galkin, V.I.: 2011, Gamma-ray and high-energy-neutron measurements on CORONAS-F during the solar flare of 28 October 2003. *Solar Phys.* **268**, 175.
Li, X., Guo, F., Chen, B., Shen, C., Glesener, L.: 2022, Modeling electron acceleration and transport in the early impulsive phase of the 2017 September 10th solar flare. *Astrophys. J.* **932**, 92.
Longcope, D.W., Beveridge, C.: 2007, A quantitative, topological model of reconnection and flux rope formation in a two-ribbon flare. *Astrophys. J.* **669**, 621. DOI. ADS.

Lysenko, A.L., Altyntsev, A.T., Meshalkina, N.S., Zhdanov, D., Fleishman, G.D.: 2018, Statistics of "cold" early impulsive solar flares in X-Ray and microwave domains. *Astrophys. J.* **856**, 111. DOI.
Metcalf, T.R., Alexander, D., Hudson, H.S., Longcope, D.W.: 2003, TRACE and Yohkoh observations of a white-light flare. *Astrophys. J.* **595**, 483. DOI. ADS.
Miklenic, C.H., Veronig, A.M., Vršnak, B., Hanslmeier, A.: 2007, Reconnection and energy release rates in a two-ribbon flare. *Astron. Astrophys.* **461**, 697. DOI. ADS.
Miklenic, C.H., Veronig, A.M., Vršnak, B.: 2009, Temporal comparison of nonthermal flare emission and magnetic-flux change rates. *Astron. Astrophys.* **499**, 893. DOI. ADS.
Miller, J.A., Cargill, P.J., Emslie, A.J., Holman, G.D., Dennis, B.R., La Rosa, T.N., Winglee, R.M., Benka, S.G., Tsuneta, S.: 1997, Critical issues for understanding particle acceleration in impulsive solar flares. *J. Geophys. Res.* **102**(A7), 14,631.
Murphy, R.J., Ramaty, R.: 1984, Solar-flare neutrons and gamma-rays. *Adv. Space Res.* **4**, 127.
Murphy, R.J., Dermer, C.D., Ramaty, R.: 1987, High-energy processes in solar flares. *Astrophys. J. Suppl.* **63**, 721.
Murphy, R.J., Kozlovsky, B., Kiener, J., Share, G.H.: 2009, Nuclear gamma-ray de-excitation lines and continuum from accelerated-particle interactions in solar flares. *Astrophys. J. Suppl.* **183**, 142. DOI. ADS.
Neupert, W.M.: 1968, Comparison of solar X-ray line emission with microwave emission during flares. *Astrophys. J.* **153**, L59.
Nita, G., Gary, D.E., Lee, J.: 2004, Statistical study of two years of solar flare radio spectra obtained with the Owens Valley Solar Array. *Astrophys. J.* **605**, 528. DOI. ADS.
Ogawara, Y., Takano, T., Kato, T., Kosugi, T., Tsuneta, S., Watanabe, T., Kondo, I., Uchida, Y.: 1991, The SOLAR-A mission – an overview. *Solar Phys.* **136**, 1. DOI. ADS.
Priest, E., Forbes, T.: 2000, *Magnetic Reconnection. MHD Theory and Applications*, Cambridge University Press, Cambridge.
Qiu, J., Hu, Q., Howard, T.A., Yurchyshyn, V.B.: 2007, On the magnetic flux budget in low corona magnetic reconnection and interplanetary coronal mass ejections. *Astrophys. J.* **659**, 758. DOI. ADS.
Qiu, J.: 2009, Observational analysis of magnetic reconnection sequence. *Astrophys. J.* **692**, 1110. DOI. ADS.
Ramaty, R., Murphy, R.J.: 1987, Nuclear processes and accelerated particles in solar flares. *Space Sci. Rev.* **45**, 213. DOI. ADS.
Sato, J., Matsumoto, Y., Yoshimura, K., Kubo, S., Kotoku, J., Masuda, S., Sawa, M., Suga, K., Yoshimori, M., Kosugi, T., Watanabe, T.: 2006, YOHKOH/WBS recalibration and a comprehensive catalogue of solar flares observed by YOHKOH SXT, HXT and WBS instruments. *Solar Phys.* **236**, 351. DOI. ADS.
Sturrock, P.A.: 1966, Model of the high-energy phase of solar flares. *Nature* **211**, 695.
Tschernitz, J., Veronig, A.M., Thalmann, J.K., Hinterreiter, J., Pötzi, W.: 2018, Reconnection fluxes in eruptive and confined flares and implications for superflares on the Sun. *Astrophys. J.* **853**, 41. DOI. ADS.
Vainio, R., Valtonen, E., Heber, B., Malandraki, O.E., Papaioannou, A., Klein, K.-L. et al.: 2013, The first SEPServer event catalogue $\sim$ 68-MeV solar proton events observed at 1 AU in 1996 – 2010. *J. Space Weather Space Clim.* **3**, A12.
Veronig, A.M., Brown, J.C., Dennis, B.R., Schwartz, R.A., Sui, L., Tolbert, A.K.: 2005, Physics of the Neupert effect: estimates of the effects of source energy, mass transport, and geometry using RHESSI and GOES data. *Astrophys. J.* **621**, 482.
Veronig, A., Polanec, W.: 2015, Magnetic reconnection rates and energy release in a confined X-class flare. *Solar Phys.* **290**, 2923.
Vilmer, N., MacKinnon, A.L., Hurford, G.J.: 2011, Properties of energetic ions in the solar atmosphere from gamma-ray and neutron observations. *Space Sci. Rev.* **159**, 167.
Watanabe, K., Muraki, Y., Matsubara, Y., Murakami, K., Sako, T., Tsuchiya, H., Masuda, S., et al.: 2003, Solar neutron event in association with a large solar flare on August 25, 2001. In: *Proc. of the 28th ICRC*, *Tsukuba, Japan*, 3179.
White, S.M., Krucker, S., Shibasaki, K., Yokoyama, T., Shimojo, M., Kundu, M.R.: 2003, Radio and hard X-ray images of high-energy electrons in an X-class solar flare. *Astrophys. J.* **595**, L111.
Zharkova, V.V., Arzner, K., Benz, A.O., Browning, P., Dauphin, C., Emslie, A., Fletcher, L., Kontar, E., Mann, G., Onofri, M., et al.: 2011, Recent advances in understanding particle acceleration processes in solar flares. *Space Sci. Rev.* **159**, 357.